Preparation and Characterization of Iron Oxide–Silica Composite Particles Using Mesoporous SBA-15 Silica as Template and Their Internalization Into Mesenchymal Stem Cell and Human Bone Cell Lines

Humphrey H. P. Yiu, Martin J. Maple, Martin R. Lees, Iryna Palona, Alicia J. El Haj, and Jon Dobson

***Abstract*—A new procedure for preparing iron oxide–silica nanocomposite particles using SBA-15 mesoporous silica as a template is described. These composite materials retained the 2-D hexagonal structure of the SBA-15 template. Transmission electron micrograms of the particles depicted the formation of iron oxide nanocrystals inside the mesochannels of SBA-15 silica framework. Powder x-ray diffraction showed that the iron oxide core of the composite particles consists of a mixture of maghemite (γ-Fe_2O_3) and heamatite (α-Fe_2O_3), which is the predominant component. Superconducting quantum interference device (SQUID) magnetometry studies showed that these iron oxide–silica composite materials exhibit superparamagnetic properties. On increasing the iron oxide content, the composite particles exhibited a stronger response to magnetic fields but a less homogeneous core, with some large iron oxide particles which were thought to be formed outside the mesochannels of the SBA-15 template. Internalization of these particles into human cell lines (mesenchymal stem cells and human bone cells), which indicates their potential in medicine and biotechnology, is also discussed.**

***Index Terms*—Internalization, iron oxide, magnetic nanoparticles, mescenchymal stem cells, mesoporous silica.**

I. Introduction

MAGNETIC micro- and nanoparticles have been shown to have great potential for applications in medicine and biology, including as contrast agents for magnetic resonance imaging (MRI) [1], drug delivery [2], gene therapy [3], and cell sorting [4]. These particles usually consist of an iron oxide core protected with a biocompatible coating, such as carbohydrate [5], protein [6], synthetic polymers [7], and silica [8]. Functionalized magnetic particles, with size range from 10 nm up to 5 μm in diameter, have been commercially available for the past decade.

Silica-coated iron oxide particles are among the most popular magnetic particles as the silica coating offers high mechanical strength along with relatively easy surface functionalization using organosilanes [9]. However, traditional routes for coating silica onto iron oxide nanoparticles usually produces heterogeneous particles with uneven coating thickness.

The highly ordered porous structures of mesoporous molecular sieves have been used as templates for many materials such as carbon [10], organic polymers [11], metal oxides [12], and metals [13]. Since the dimensions of the core materials are highly regulated by the pore size, potential applications of these nanomaterials include fuel cell technology [14], nanoelectronics [15], and biotechnology [16].

With a network of highly ordered channels of 2–10 nm in diameter, these mesoporous molecular sieves can be used as a template for preparing metal oxide–silica composite materials with a high degree of control over the particle size [17], [18]. Also, because the particles have a large pore volume, a high loading of metal oxide can be achieved.

In this work, a new technique for preparing iron oxide–silica composite nanoparticles with high iron oxide content using SBA-15 mesoporous silica as template is reported. Because of the ultrahigh pore volume (ca. 1 $cm^3\ g^{-1}$) of these silica materials [19], theoretically the iron content of the composite can be increased up to 83% by weight (estimated from the pore volume of SBA-15 and the density of iron oxide ca. 5 g cm^{-3}). In order to explore their applications in medicine and biology, internalization of these composite particles into mescenchymal stem cells and human bone cells is also studied in this work.

II. Experimental

A. Preparation of the SBA-15 Template and Impregnation of the Iron Oxide Core

Descriptions of preparation procedures for pure siliceous SBA-15 ordered mesoporous silica materials are widely available in the literature [20]. Pluronic P123 triblock copolymer (EO_{-20}-PO_{70}-EO_{20}, BASF) was used as a surfactant template. A typical reaction composition in molar ratio was 1 SiO_2: 0.017 P123: 2.9 HCl: 202.6 H_2O. The surfactant Pluronic P123 was dissolved in a mixture of water and HCl at 40°C.

Manuscript received June 17, 2008; accepted September 30, 2009. Date of publication July 08, 2010; date of current version September 01, 2010. This work was supported by the BBSRC. The work of J. Dobson was supported by a Royal Society Wolfson Research Merit Award. *Asterisk indicates corresponding author.*

J. Dobson and A. J. El Haj are with the Institute of Science and Technology in Medicine, Keele University, Stoke-on-Trent, ST4 7QB, U.K. (e-mail: bea22@keele.ac.uk).

H. H. P. Yiu was with the Institute of Science and Technology in Medicine, Keele University, Stoke-on-Trent, ST4 7QB, U.K.. He is now with the Department of Chemistry, University of Liverpool, Liverpool, L69 7ZD, U.K. (e-mail: h.yiu@liv.ac.uk).

M. J. Maple is with the School of Applied Science, University of Wolverhampton, Wolverhampton, WV1 1LY, U.K.. (e-mail: m.j.maple@wlv.ac.uk).

M. R. Lees is with the Department of Physics, University of Warwick, Coventry, CV4 7AL, U.K. (e-mail: m.r.lees@warwick.ac.uk).

Digital Object Identifier 10.1109/TNB.2010.2053770

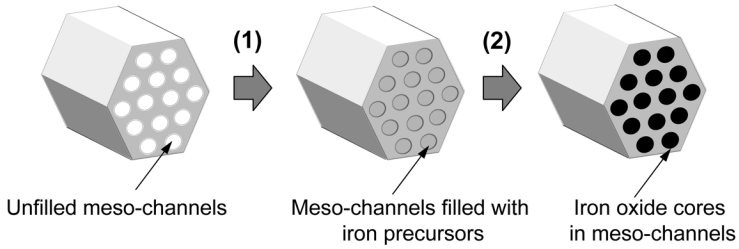

Fig. 1. A schematic showing the preparation procedure of iron oxide–silica nanocomposite using SBA-15 mesoporous silica particles as templates.

Tetraethylorthosilicate (98%, Aldrich) was added to the surfactant solution and the mixture was stirred for 24 h at 30°C. A white suspension formed after 24 h and the reaction mixture was then transferred to a Teflon bottle and heated at 100°C for 2 days. The resulting white precipitates were filtered and washed with distilled water then air dried. The surfactant template was removed by calcination under a flowing nitrogen stream at 550°C for 4 h, then followed by oxygen at the same condition.

Iron(III) oxide particles were incorporated inside the mesochannels of SBA-15 via wet impregnation followed by thermal decomposition. Calcined SBA-15 particles (1 g) were suspended in 5 cm^3 of hydrated iron(III) nitrate ($Fe(NO_3)_3{\cdot}9H_2O$, 99%, Aldrich) ethanolic solution for 1 h. Various amount of $Fe(NO_3)_3$ was used in order to prepare composite materials with 10%, 33%, and 50% w/w iron oxide. The suspension was then allowed to dry at 40°C while stirring continued. The dried particles were then heating to 300°C at a heating rate of 10°C min^{-1}. The resultant solid was brown in color and the intensity of color directly related to the iron content. The samples were characterized using powder XRD (Philips), superconducting quantum interference device (SQUID) magnotometry (Quantum Designs MPMS) and high-resolution transmission electron microscopy (TEM) (JEOL 120 keV).

Prior to cell experiments, Fe_2O_3-SBA-15 particles were suspended in sterile water at a concentration of 5 mg per cm^3 and stored under UV radiation overnight for sterilization.

B. Cell Culture, Cytotoxicity, and Internalization of Iron Oxide–Silica Composite Particles

The cytotoxicity of Fe_2O_3-SBA-15 was tested using WST-8 assay (Sigma). E14 mouse embryonic stem (mES) cells were used in this cytotoxicity assay. Cells were grown and maintained using high glucose advanced culture medium supplemented with 2% fetal calf serum (ES-grade), 1000 U cm^{-3} Leukemia Inhibitory Factor (LIF), 5 μM mercaptoethanol, and 2 mM L-glutamine. For cytotoxicity assays, cells were seeded at 100000 cells per well in a 96 well tissue culture plate in 0.1 cm^3 medium and cultured overnight at 37°C 5%CO_2. At 24 h post seeding, 200 ng of composite material was added to each well. After 96 h, 10×10^{-3} cm^3 (or 10 μL) of WST-8 was added to the wells and incubated for 4 h. The absorbance at 450 nm developed was then quantified using a Spectra Max Plus spectrometer (Medical Devices). The cell viability was calculated against the control experiment without addition of composite materials with $n = 6$.

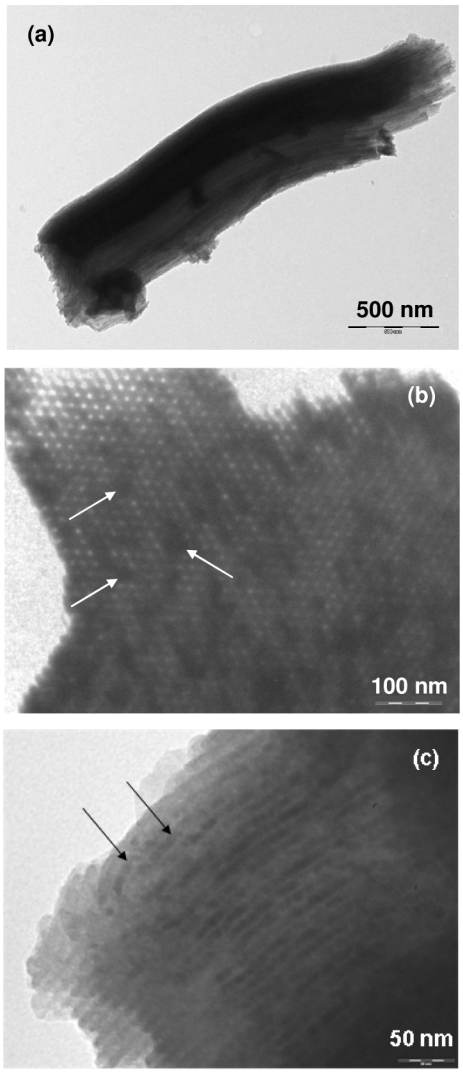

Fig. 2. TEM microgram of iron oxide–silica nanocomposites (33%) materials. Fig. 2(a) shows a typical nanocomposite particle, while Fig. 2(b) shows the 2-D hexagonal structure was retained. In Fig. 2(b) and 2(c), the iron oxide particles, indicated by arrows (→), are found inside the mesochannels of the SBA-15 framework.

In the internalization study, iron oxide–silica nanocomposite particles were loaded into mesenchymal stem cells MSC [MSCs of a male patient were obtained from Lonza (Lonza Walkersville, MD)] and the human osteoblast cells line, MG-63 [American Tissue Culture Collection (ATCC)]. The cells were seeded at 10 000 cells per dish (at 2500 cells per cm^3 of media) and cultured with low glucose DMEM medium (Biosera) containing 10% fetal calf serum (Biosera), 1% antibiotics and 1% L-glutamate at 37°C with flowing CO_2 at 5 $cm^3 min^{-1}$. After 24 h in culture, 20 ng of particles (with serial dilutions in sterile

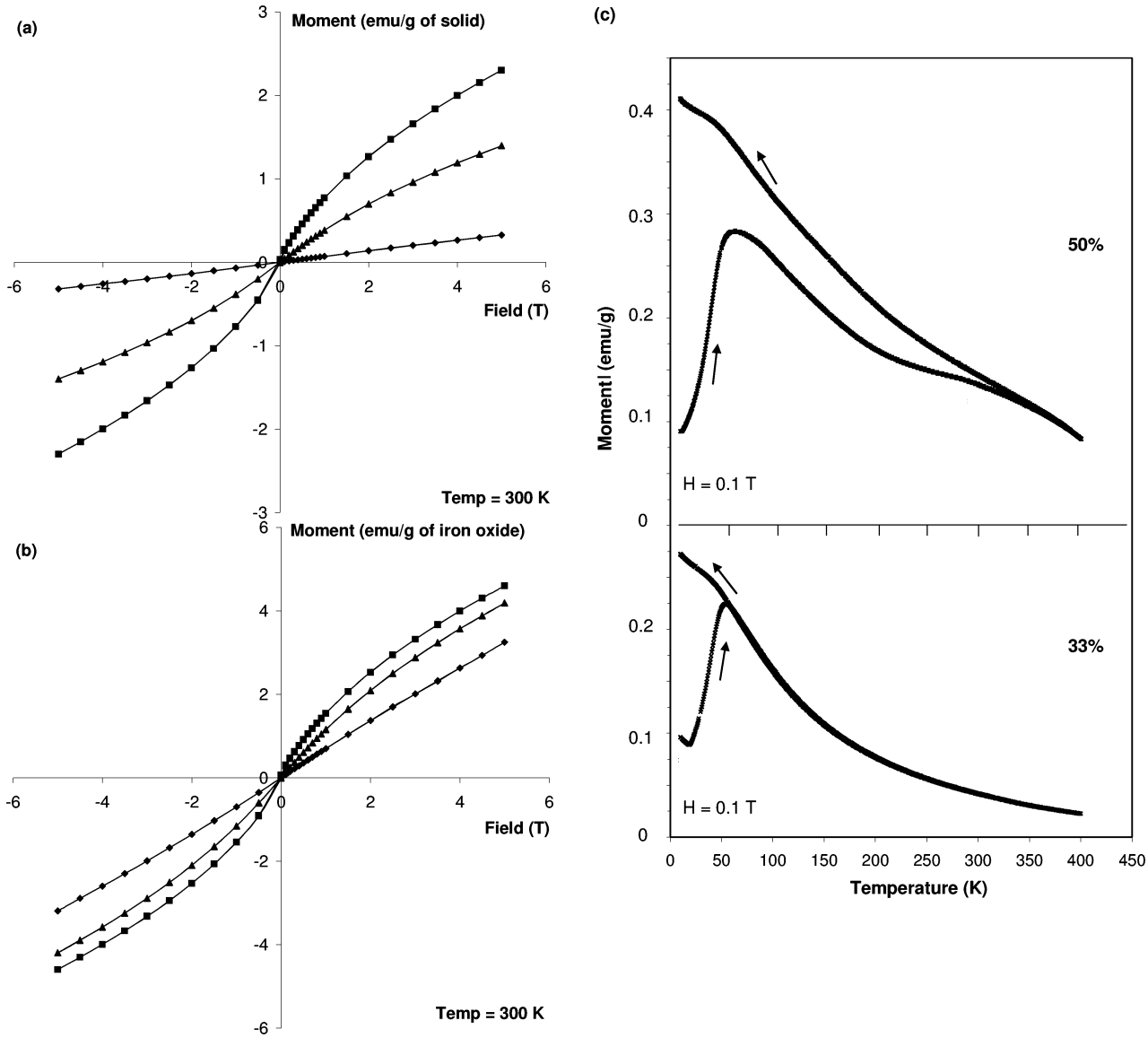

Fig. 3. Results from SQUID magnetometry measurements. (a) M versus H plots of iron oxide–silica nanocomposites (10%, 33%, and 50% iron oxide) at Temp.= 300 K. (b) M versus H plots normalized to unit of iron content. (c) ZFC/FC curves for iron oxide–silica nanocomposites (33% and 50% iron oxide) measured at H= 0.1 T.

water) was added into 2 cm^3 serum-free (SF) low glucose DMEM medium. The cells were then incubated at 37°C in a humidified atmosphere at 5% CO_2 for 24 h and followed by fixation using 4% formaldehyde (Sigma) in phosphated saline buffer (PBS) solution for 15 min. Finally, the cells were dyed with Hematoxylin followed by Eosin Y solution (Sigma) in order to provide good contrast for imaging. Three dishes of cells were used for both cell lines. An Olympus XI-71 light microscope was used to observe any internalization of particles into cells and captured using a digital camera ColorView III (Olympus) interfaced with Cell-B software.

III. Results and Discussion

A. Characterization of Iron Oxide-Silica Composite Particles

The calcined SBA-15 showed a typical p6 mm structure with a 2-D hexagonal array of parallel channels of diameter at around 6 nm (estimated from TEM images). Impregnation of iron oxide was then carried out using these particles. Fig. 1 illustrates the impregnation process of an iron oxide core into SBA-15 silica template.

After the temperature-programmed decomposition (TPD), brown powder was formed and the intensity of the color depended on the iron content. Fig. 2(a) shows a TEM image of an iron oxide–silica nanocomposite (33% w/w), while Fig. 2(b) shows that the 2-D hexagonal structure of SBA-15 was retained. The magnetic core was formed by iron oxide nanocrystals embedded inside the channels and these nanocrystals have a diameter of around 5 nm due to the dimensions of the channels inhibiting their growth during decomposition [Fig. 2(c)]. From the TEM images, some unfilled mesoporous cavities were seen inside the particles, so it appears possible that the iron oxide content may be further increased. Measurements of the pore volume of SBA-15 are widely available in the literature and it is generally accepted that the particles have a pore volume of around 1 cm^3 per gram of silica. When these channels are

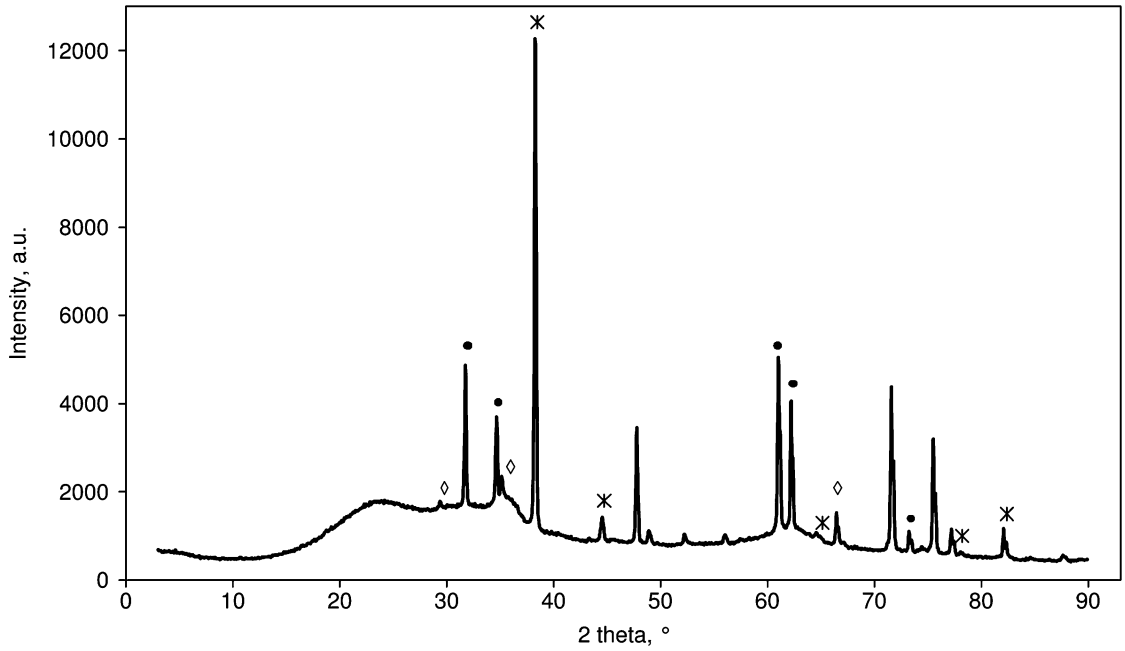

Fig. 4. Powder x-ray diffraction pattern of iron oxide–silica nanocomposite particles (33%). Peaks marked with (◇) are corresponding to γ-Fe_2O_3 (maghemite) while those for α-Fe_2O_3 (heamatite) are marked with (•). The broad peaks at 20–40 and around 60 degrees are due to the amorphorous silica of SBA-15. Peaks marked with (*) are due to the aluminium sample holder. A schematic showing the preparation procedure of iron oxide–silica nanocomposite using SBA-15 mesoporous silica particles as templates.

completely fill up with iron oxide (density of 4.8–5.1 g cm^{-3}), the maximum amount of iron oxide in the composite will be around 5 g, which gives an iron oxide content of ca. 83% w/w. However, this high content can be difficult to achieve, and a very precise impregnation protocol is needed. A typical particle size was estimated to be ca. 500 nm–2 μm.

The size of the iron oxide nanocrystals can also be increased by using a mesoporous silica template with a larger pore size. Increasing the pore size of SBA-15 can be achieved by adding a swelling agent (such as mesitylene) to increase the dimension of the micelles during synthesis. Increasing the size of iron oxide nanocrystals can increase the response of the composite materials to a magnetic field. This mechanism can increase the pore size of mesoporous silica up to 30 nm. Unfortunately, increasing the amount of the swelling agent also causes loss of structural order and reduction in pore volume (hence reducing the maximum loading of iron oxide).

The magnetic properties of the particles were studied using SQUID magnetometry. The M versus H plots performed at temperature $=$ 300 K [Fig. 3(a)] for these composite samples showed superparamagnetic behavior and the magnetic response increased with increasing iron oxide content. Saturation was not achieved, and this is likely due to the presence of high-coercivity hematite as the dominant iron oxide phase.

Composite particles with 10% w/w iron oxide content exhibited a very low magnetic susceptibility with no obvious saturation. As the iron oxide content increased, susceptibility increased proportionally. Fig. 3(b) was plotted after normalizing the weight of iron oxide in these three nanocomposite samples. Higher iron content in the composite clearly gives materials with stronger magnetic response. A possible reason for this phenomenon is the formation of larger iron oxide crystals with an increased iron content.

Zero field cooled/field cooled (ZFC/FC) measurements, ($B = 0.1$ T) [Fig. 3(c)] for the particles with 33% w/w iron oxide show a distinct blocking temperature peak at ∼60 K and superposition of the curves at the same temperature, giving and indication that the particle size of the magnetic iron oxide is uniform. At higher concentrations (50% w/w iron oxide) the mean blocking temperature is shifted slightly, to ∼80 K and there is separation of the two curves up to 320 K, indicating a broad range of particles sizes, with some particles being blocked at room temperature. This is likely to be due to the formation of larger iron oxide particles outside the channels. To avoid the formation of large iron oxide particles outside the mesochannels, repeating impregnation at a smaller amount each time may give a more evenly distributed iron oxide content throughout the SBA-15 template.

Powder XRD of composite particles with 33% w/w iron oxide showed the iron oxide core in all samples consists of a mixture of α-Fe_2O_3 (heamatite) and γ-Fe_2O_3 (maghemite), with α-Fe_2 O_3 being the majority [Fig. 4(a)]. These results are consistent with the magnetometry data and any significant amounts of maghemite would saturate at low fields. This is not observed in the M versus H curves. Fig. 4(b) and (c) are standard x-ray diffraction patterns for heamatite and maghemite.

This work has demonstrated that magnetic iron oxide–silica composites can be prepared by thermal decomposition of iron(III) oxy-salt such as nitrate. However, it is difficult to control the formation of α-Fe_2O_3, which is antiferromagnetic. To increase the response of the composite to an external magnetic field, the iron(III) oxide particles of the composite can be reduced to iron(II, III) oxide (Fe_3O_4) or magnetite, using a temperature-programmed reduction (TPR). Research on the formation of magnetite–silica composite from this protocol is currently being carried out.

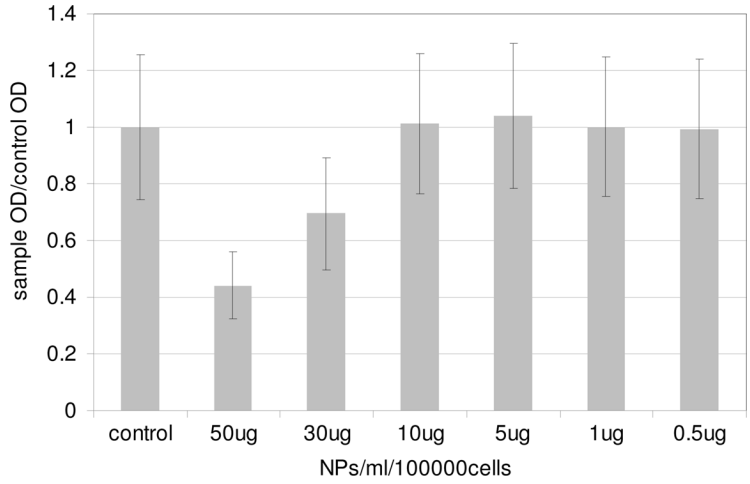

Fig. 5. Cytotoxicity assay for Fe_2O_3-SBA-15 particles using mouse embryonic stem cells $(n = 6)$.

B. Internalization of Iron Oxide-Silica Composite Particles Into Human Cell Lines

These composite particles have already shown potentials in some biomedical applications such as gene delivery [3] and drug delivery [2]. In this case, examining the internalization process of particles is essential in order to ensure the viability of cells and to examine the potential toxicity of the particles. The viability of most cells was not affected after particle internalization. From the viability test using mouse embryonic stem cell, there was no toxicity effect observed up to a dose of 10 μg cm^{-3} per 100 000 cells (see Fig. 5). Cell viability decreases as the dose increases from 30 μg to 50 μg cm^{-3}. Fig. 6 depicts mesenchymal stem cells [Fig. 6(a)] and human osteoblast cells [Fig. 6(b)] containing internalized with iron oxide–silica (33% w/w) composite particles.

This gives a good indication that this process may be developed for the production of magnetic particles for cell targeting, as the cells can be driven by a magnetic field after internalization of the magnetic particles. Preliminary studies in our laboratory have shown that the cells with internalized iron oxide–silica composite particles are responsive to an external magnetic field.

The composite particles we used in this work only consist of an array iron oxide cores and a hexagonal silica framework. To improve the biocompatibility of the particles, the surface can be further functionalized with peptides, lipids, or carbohydrates with organic linkers. With a biocompatible surface, specific functionalization such as tagging with antibodies or DNA is relatively straightforward.

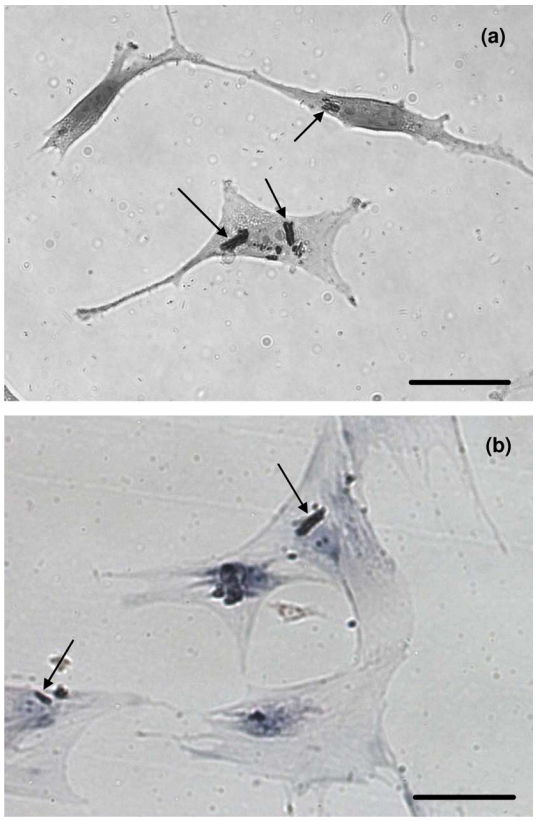

Fig. 6. Microscopic images of: (a) human osteoblast cells MG-63 and (b) mesenchymal stem cells after internalizing iron oxide–silica nanocomposite particles (indicated by →). The scale bars in both figures are equivalent to 10 μm.

IV. Conclusion

A new method of preparing superparamagnetic iron oxide–silica composite particles has been demonstrated. The magnetic susceptibility of the nanocomposite particles to an external magnetic field increases as the iron oxide content increases. From the powder XRD results, the iron oxide core was found to be a mixture of maghemite and hemaetite, which is the predominant component. TEM images showed the nanostructure of these particles consists of the 2-D hexagonal silica framework with iron(III) oxide nanocrystals of around 5 nm in diameter inside the mesochannels of SBA-15. Internalization of these magnetic particles into living cells was demonstrated and the particles did not prove to be particularly toxic to the cells. These particles appear to have potential to be used for magnetic delivery and targeting of cells *in vivo* as well as for cell sorting and the magnetic actuation of cellular functions through targeted attachment of the particles to cells in culture and in the body—particularly if more magnetic magnetite and maghemite phases can be created and maintained.

References

[1] S. Mornet, S. Vasseur, F. Grasset, and E. Duguet, "Magnetic nanoparticle design for medical diagnosis and therapy," *J. Mater. Chem.*, vol. 14, pp. 2161–2175, Jul. 2004.

[2] Q. A. Pankhurst, J. Connoly, S. K. Jones, and J. Dobson, "Applications of magnetic nanoparticles in biomedicine," *J. Phys. D.*, vol. 36, pp. R167–R181, Jul. 2003.
[3] J. Dobson, "Magnetic nanoparticle-based gene delivery," *Gene Therapy*, vol. 13, pp. 283–287, Feb. 2006.
[4] L. P. Sun, M. Zborowski, L. R. Moore, and J. J. Chalmers, "Continuous, flow-through immunomagnetic cell sorting in a quadrupole field," *Cytometry*, vol. 33, pp. 469–475, Dec. 1998.
[5] L. M. Lacava, Z. G. M. Lacava, M. F. Da Silva, O. Silva O, S. B. Chaves, R. B. Azevedo, F. Pelegrini, C. Gansau, N. Buske, D. Sabolovic, and P. C. Morais, "Magnetic resonance of a dextran-coated magnetic fluid intravenously administered in mice," *Biophys. J.*, vol. 80, pp. 2483–2486, May 2001.
[6] A. R. Simioni, O. P. Martins, Z. G. M. Lacava, R. B. Azevedo, E. C. D. Lima, B. M. Lacava, P. C. Morais, and A. C. Tedesco, "Cell toxicity studies of albumin-based nanosized magnetic beads," *J. Nanosci. Nanotechnol.*, vol. 6, pp. 2413–2415, Aug. 2006.
[7] F. Caruso, M. Spasova, A. Susha, M. Giersig, and R. A. Caruso, "Magnetic nanocomposite particles and hollow spheres constructed by a sequential layering approach," *Chem. Mater.*, vol. 13, pp. 109–116, Jan. 2001.
[8] S. Santra, R. Tapec, N. Theodoropoulou, J. Dobson, A. Hebard, and W. H. Tan, "Synthesis and characterization of silica-coated iron oxide nanoparticles in microemulsion: The effect of nonionic surfactants," *Langmuir*, vol. 17, pp. 2900–2906, May 2001.
[9] J. H. Clark and D. J. Macquarrie, "Catalysis of liquid phase organic reactions using chemically modified mesoporous inorganic solids," *Chem. Commun.*, pp. 853–860, Apr. 1998.
[10] R. Ryoo, S. H. Joo, and S. Jun, "Synthesis of highly ordered carbon molecular sieves via template-mediated structural transformation," *J. Phys. Chem. B*, vol. 103, pp. 7743–7746, Sep. 1999.
[11] M. S. Cho, H. J. Choi, and W. S. Ahn, "Enhanced electrorheology of conducting polyaniline confined in MCM-41 channels," *Langmuir*, vol. 20, pp. 202–207, Jan. 2004.
[12] H. F. Yang, Q. H. Shi, B. Z. Tian, Q. Y. Lu, F. Gao, S. H. Xie, J. Fan, C. Z. Yu, B. Tu, and D. Y. Zhao, "One-step nanocasting synthesis of highly ordered single crystalline indium oxide nanowire arrays from mesostructured frameworks," *J. Amer. Chem. Soc.*, vol. 125, pp. 4724–4725, Apr. 2003.
[13] W. P. Zhu, Y. C. Han, and L. J. An, "Silver nanoparticles synthesized from mesoporous Ag/SBA-15 composites," *Microporous Mesoporous Mater.*, vol. 80, pp. 221–226, May 2005.
[14] X. He and D. Antonelli, "Recent advances in synthesis and applications of transition metal containing mesoporous molecular sieves," *Angew. Chem. Int. Ed.*, vol. 41, pp. 214–229, Jan. 2002.
[15] E. Chomski and G. A. Ozin, "Panoscopic silicon—A material for "all" length scales," *Adv. Mater.*, vol. 12, pp. 1071–1078, Jul. 2000.
[16] H. H. P. Yiu and P. A. Wright, "Enzymes supported on ordered mesoporous solids: A special case of an inorganic-organic hybrid," *J. Mater. Chem.*, vol. 15, pp. 3690–3700, 2005.
[17] S. C. McBain, H. H. P. Yiu, A. J. El Haj, and J. Dobson, "DNA delivery using polyethylenimine (PEI) coated iron oxide–silica mesostructured particles," *Stud. Surf. Sci. Catal.*, vol. 165, pp. 869–872, Jul. 2007.
[18] H. H. P. Yiu, S. C. McBain, A. J. El Haj, and J. Dobson, "A triple-layer design for polyethyleneimine-coated, nanostructured magnetic particles and their use in DNA binding and transfection," *Nanotechnology*, vol. 18, p. 435601, Oct. 2007.
[19] M. Kruk, M. Jaroniec, C. H. Ko, and R. Ryoo R, "Characterization of the porous structure of SBA-15," *Chem. Mater.*, vol. 12, pp. 1961–1968, Jul. 2000.
[20] H. H. P. Yiu, P. A. Wright, and N. P. Botting, "Enzyme immobilisation using siliceous mesoporous molecular sieves," *Microporous Mesoporous Mater.*, vol. 44–45, pp. 763–768, Jun. 2001.
[21] T. Kinoshita, S. Seino, K. Okitsu, T. Nakayama, T. Nakagawa, and T. A. Yamamoto, "Magnetic evaluation of nanostructure of gold-iron composite particles synthesized by a reverse micelle method," *J. Alloys Compounds*, vol. 359, pp. 46–50, Sep. 2003.

Authors' photographs and biographies not available at the time of publication.